Supplementary Information

From metastability to equilibrium during the sequential growth of Co-Ag supported clusters: a real-time investigation

Pascal Andreazza[1*], *A. Lemoine*[1,2], *A. Coati*[2], *D. Nelli*[3], *R. Ferrando*[3], *Y. Garreau*[2,4], *J. Creuze*[5], *C. Andreazza-Vignolle*[1]

**Corresponding Author pascal.andreazza@univ-orleans.fr*

1 Université d'Orléans, CNRS, ICMN UMR7374, 1b rue de la Férollerie, F-45071 Orléans, France
2 Synchrotron SOLEIL, L'Orme de Merisiers, F-91192 Gif-sur-Yvette, France
3 Università di Genova, Dipartimento di Fisica, Via Dodecaneso 33, Genova, I16146, Italy
4 Université de Paris, CNRS, Laboratoire Matériaux et Phénomènes Quantiques UMR7162, F-75013 Paris, France,
5 Université Paris-Saclay, CNRS, ICMMO UMR8182, F-91405 Orsay, France

TEM image

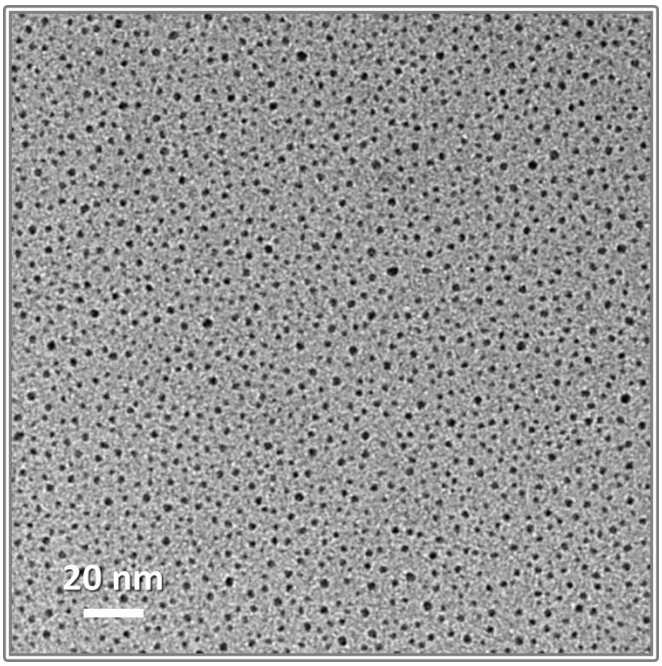

Figure S1 : TEM transmission electron microscopy image of the initial Ag NPs obtained by UHV vapor deposition at room temperature (RT) on amorphous-C/SiO_2/Si(100) substrate, performed in the same procedure than [1].

Synchrotron radiation experiments

In-situ Grazing Incidence Small Angle X-ray Scattering (GISAXS) and Grazing Incidence Wide Angle X-ray Scattering (GIWAXS) measurements were carried out at the SOLEIL Synchrotron in Gif-sur-Yvette, France, at the SIXS beamline [2,3]. The photon energies of 7.7 KeV or 16 KeV were used in the two different campaigns with an angle of incidence fixed at 0.18° and 0.08° respectively to optimize the analysis depth to some nanometers (fig. S2). The energy range around 7.7KeV was chosen close to the K absorption edge of Co, while the energies of the Ag absorption edges were not accessible in this beam line. The sample detector distance was chosen for each x-ray energy to adjust the q range of the collected signal in the reciprocal space. All GIWAXS signals were collected with a Cyberstar photon point detector, at 16 KeV and with an XPAD 2D detector with dimensions of 240 x 560 pixels and a pixel size of 130x130 μm^2. The 2D detector used for the GISAXS measurements was a Mar CCD detector, with dimensions of 2048 x 2048 pixels and a pixel size of 80x80 μm^2 located at 600mm and 1260mm of the sample at 7.7 KeV and 16 KeV, respectively. The GISAXS and GIWAXS detectors were calibrated in terms of detection uniformity, spatially and energetically.

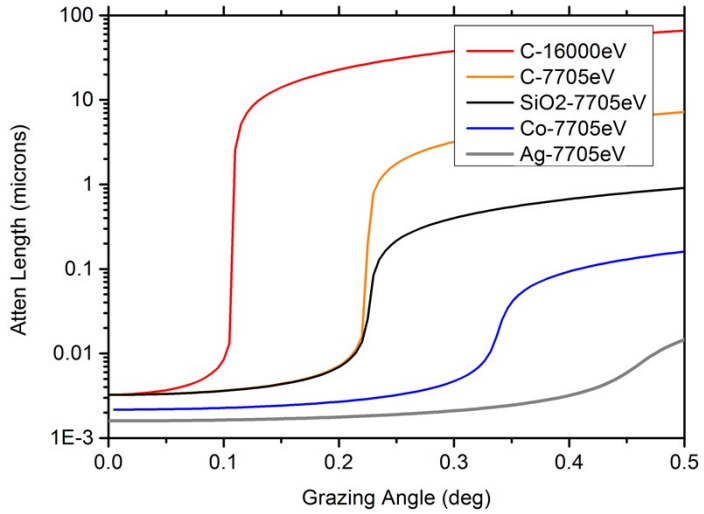

Figure S2: Attenuation length of X-ray beam with the grazing incidence for silica, Ag and Co at 7.7 KeV and for amorphous carbon at 7.7 KeV and 16 KeV.

The geometry of the scattering data collection is defined at a fixed grazing incidence α_i [4, 5, 6]: The scattered intensity is recorded as a function of the out-of-plane angle α_f with respect to the substrate surface and of the in-plane angle $2\theta_f$ (Fig. 1a). For GIWAXS, the exit angle α_f is fixed and the scan angle is $2\theta_f$. The components of the momentum transfer $\mathbf{q} = \mathbf{k_i} - \mathbf{k_f}$, (scattering vector) defined by the incident k_i and the scattered k_f wave vectors are $q_x = k_i (\cos\alpha_f \cos 2\theta_f - \cos\alpha_i)$, $q_y = k_i (\cos\alpha_f \sin 2\theta_f)$ and $q_z = k_i (\sin\alpha_f + \sin\alpha_i)$ in the laboratory frame, x and y in the surface substrate plane and z out-of plane (y perpendicular to the incident beam). For GISAXS, the intensity is recorded in q_y and q_z on the 2D detector.

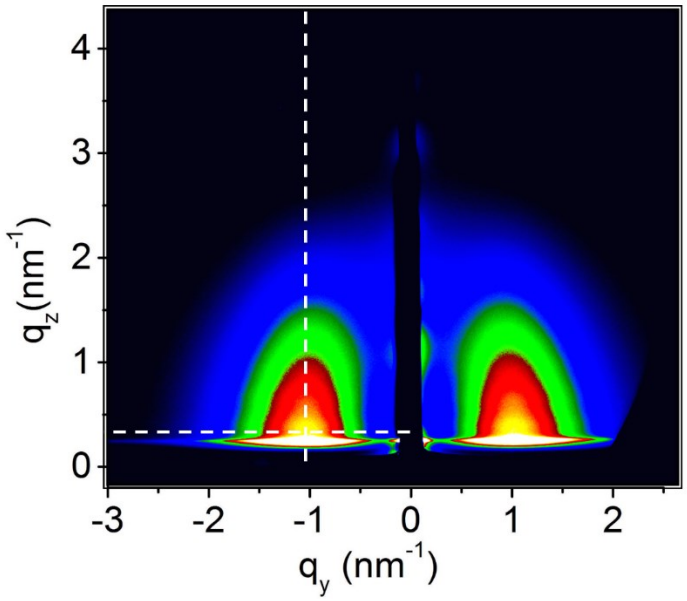

Figure S3: Representative 2D GISAXS pattern of the AgCo NPs (intensity in log scale). The q_y (resp. q_z) axis is parallel (resp. perpendicular) to the sample plane and the one-dimensional q_y and q_z cuts are showed by the white dashed lines.

X-ray scattering Analysis procedure

For GISAXS data analysis: two cuts of intensity, *i.e.* 1D profiles, in the (b) q_z and (c) q_y directions (see figure 1b-c), were extracted from a 2D GISAXS pattern as shown in Figure S3 as in ref.[7]. The two perpendicular experimental cuts (marks) selected in the lobe intensity region (dashed lines) in Figure S3 were simultaneously fitted with a dedicated code, IsGISAXS software [5]. The calculations were based on the Distorted Wave Born Approximation (DWBA) theory, because of the X-ray reflection effect in grazing configuration in incidence and emergence. The simulations were made for a distribution of weakly-truncated spherical shape of nanoparticles, to consider of the weak interactions between the deposited metals and the substrate. According to the NPs organization on the substrate, the inter-particles correlation function was calculated using the Local Monodisperse Approximation (LMA), and a 1D-paracrystal organization model [7,8]. The adjustable parameters of the simulations were the NPs diameter D, the aspect ratio H/D (where H is the NPs height), the relative distribution of diameter $\sigma(D)/D$, the inter-particles distance Λ, and its standard deviation $\sigma(\Lambda)/\Lambda$ [9,4].

For GIWAXS data analysis: the 1D experimental scattering profile was compared with simulated pattern obtained from calculated model cluster on the basis of the Debye equation [6,4] and considering the set-up geometry using a dedicated home-made software [10]. Preliminarily, a reference pattern from a substrate region without particle was measured in the same conditions and in non-anomalous measurement, and was subtracted to the deposited nanoparticle sample pattern. The model clusters were obtained from Monte Carlo (MC) simulations with atomic displacements and chemical species exchanges of Co and Ag atoms in the canonical ensemble, using a semi-empirical tight-binding potential. A weighted sum of the intensities from several sizes or structures was used to fit the WAXS patterns considering the size distribution coming from GISAXS results.

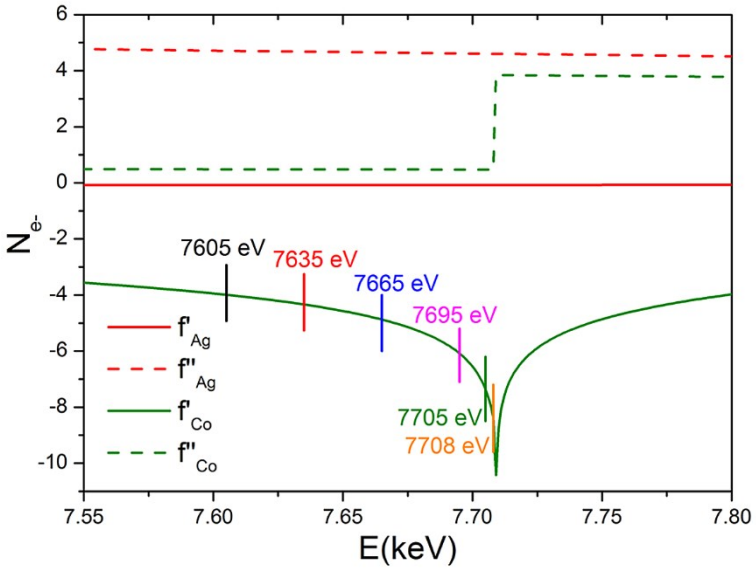

Fig S4 : Anomalous variation of the atomic scattering factor terms (in number of electrons) depending on the x-ray energy for Ag and Co close to the Co K edge.

For anomalous scattering, the measurements were based on the atomic scattering factor variations, around an X-Ray absorption edge [11, 12, 13]. Basically, the scattered intensity expression for CoAg bi-metallic NPs is:

$$I(q,E) = |f_{Co}(q,E)|^2 S_{CoCo}(q) + |f_{Ag}(q,E)|^2 S_{AgAg}(q) + \left(f_{Co}(q,E) f_{Ag}^{*}(q,E) + f_{Ag}(q,E) f_{Co}^{*}(q,E)\right) S_{CoAg}(q)$$

where q is the scattering vector, E is the X-ray energy, $S_{MN}(q)$ is the Partial Structure Factor (PSF) that represents the atomic pair correlation functions and thus provides the inter-atomic first neighbors distances thanks to a Fourier transform. f_M are the atomic scattering factors of Co an Ag atoms. In particular, $f_M(q,E) = f_{0M}(q) + f_M'(E) + i f_M''(E)$ where $f_{0M}(q)$ represents the atomic form factor for the M type atom which is the Fourier transform of the atomic electron density. $f'(q,E)$ and $f''(q,E)$ are the real and imaginary part of the dispersion correction which represent the atomic dissipation and absorption of the incident electromagnetic wave (figure S4).

Faraway of the absorption edge of the considered element, $f'(q,E)$ and $f''(q,E)$ evolutions with respect to the X-ray energy are negligible, so they were considered as constant. However, near the absorption edge, these terms vary significantly, and strongly modify the scattering signal [11, 14]. Considering the case of our bimetallic system containing elements Co and Ag: as the anomalous scattering is performed around the absorption edge of the Co element, only the atomic scattering factor of this metal will be affected. Thus, performing a subtraction between the scattering spectra realized at least for two different energies (E_1 and E_2), the expression of the remaining scattering signal is:

$$\Delta I_{Co}(q) = I(q,E_2) - I(q,E_1)$$

Thanks to the intensity subtraction ΔI analysis, called the "differential method" [14] at the Co K edge (one edge at least), the contributions to the scattering signal of pairs Ag-Ag were eliminated, whereas Co-Co and Co-Ag atomic pairs contributions were not negligible. Thus, A-GIWAXS method provided a selective access to Co atoms structural environment, and allowed investigating the chemical configuration of the NPs.

GIWAXS spectra during the Co deposition

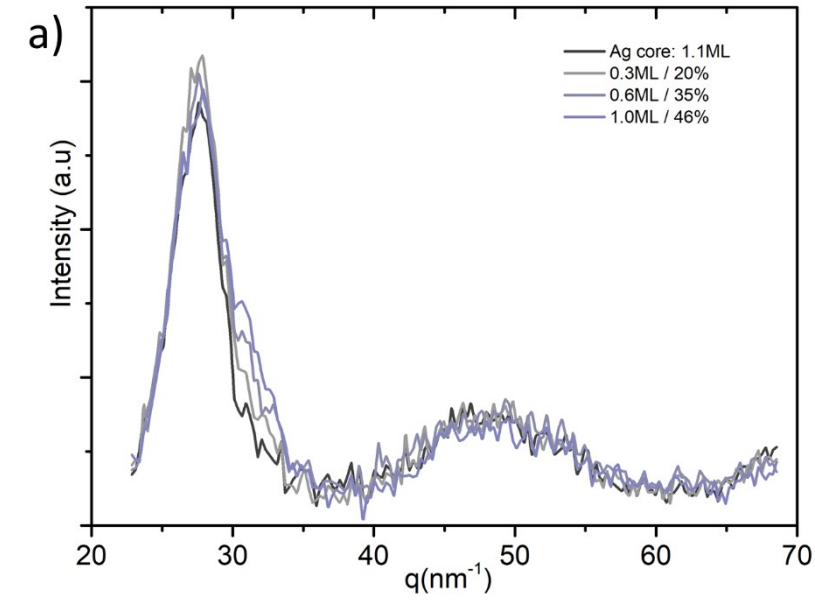

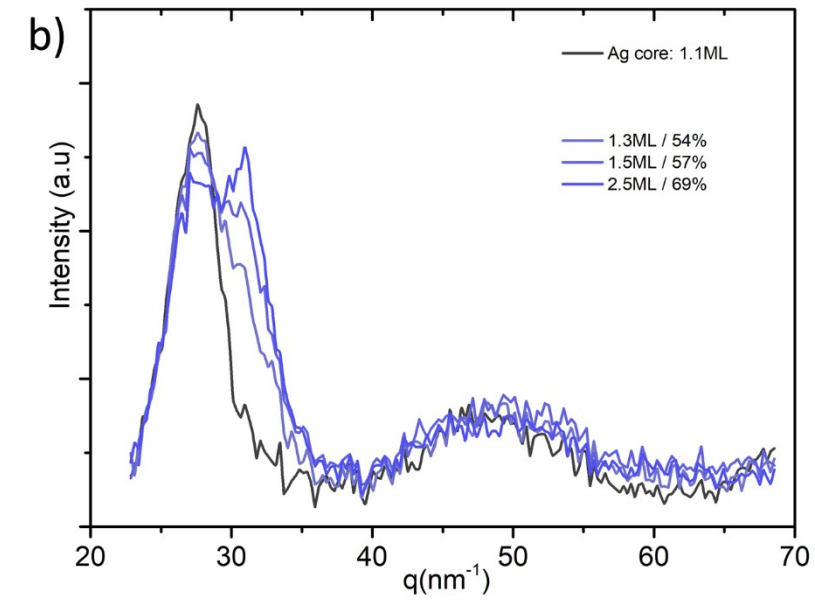

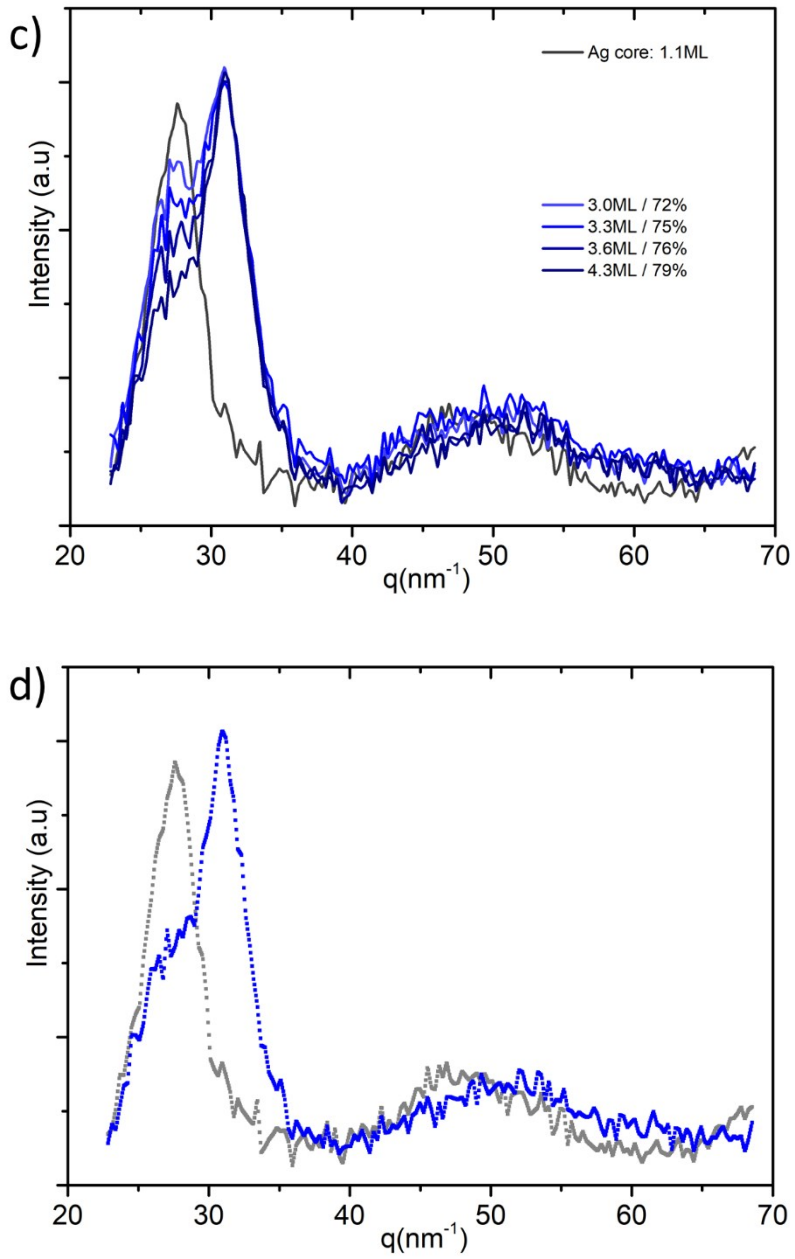

Figure S5 : GIWAXS spectra from the Figure 4b) as a function of deposited amount of Co atoms, separated in 3 groups a), b) and c) for a better view. d) GIWAXS spectra of Ag clusters at the end of Ag deposition and Co-Ag at the end of the Co deposition for 80% Co atoms. The initial spectrum of the Ag clusters before Co deposition is on all figures in dark grey.

References

[1] Penuelas, J., Andreazza-Vignolle, C., Andreazza, P., Ouerghi, A., Bouet, N. Temperature effect on the ordering and morphology of CoPt nanoparticles. Surf. Sci. 602, 545–551 (2008).
[2] Wilson, A., Bernard, R., Vlad, A., Borensztein, Y., Coati, A., Croset, B., Garreau, Y., Prévot, G. "Epitaxial growth of bimetallic Au-Cu nanoparticles on TiO2(110) followed in situ by scanning tunneling microscopy and grazing-incidence x-ray diffraction" Physical Review B., 90(7): 075416. (2014).

[3] Coati, A., Chavas, L. M. G., Fontaine, P., Foos, N., Guimaraes, B., Gourhant, P., Thompson, A. (2017). Status of the crystallography beamlines at synchrotron SOLEIL⋆ . The European Physical Journal Plus, 132(4).
[4] Andreazza P. (2012) Probing Nanoalloy Structure and Morphology by X-Ray Scattering Methods. In: Alloyeau D., Mottet C., Ricolleau C. (eds) Nanoalloys. Engineering Materials. Springer, London DOI:10.1007/ 978-1-4471-4014-6_3
[5] Lazzari, R. IsGISAXS: a program for grazing-incidence small-angle X-ray scattering analysis of supported islands. J. Appl. Crystallogr. 35, 406–421 (2002).
[6] Penuelas, J., Andreazza, P., Andreazza-Vignolle, C., Tolentino, H.C.N., De Santis, M., Mottet, C.: Controlling structure and morphology of CoPt nanoparticles through dynamical or static coalescence effects. Phys. Rev. Let. 100(11), 115502 (2008)
[7] Andreazza, P., Mottet, C., Andreazza-Vignolle, C., Penuelas, J., Tolentino, H.C.N., De San-tis, M., Felici, R., Bouet, N.: Probing nanoscale structural and order/disorder phase transitions of supported Co-Pt clusters under annealing. Physical Review B 82(15), 155453 (2010).
[8] Leroy, F., Lazzari, R., Renaud, G.: Effects of near-neighbor correlations on the diffuse scattering from a one-dimensional paracrystal. Acta Crystallographica Section A 60, 565-581 (2004).
[9] Renaud, G., Lazzari, R., Leroy, F.: Probing surface and interface morphology with Grazing Inci-dence Small Angle X-Ray Scattering. Surf. Sci. Rep. 64(8), 255-380 (2009).
[10] Virot L., Andreazza P. (2006) XDSS Software, Orléans, France
[11] Lemoine, A., Kataya, Z., Andreazza, P., Garreau, Y, Andreazza-Vignolle, C., Coati, C., From core-shell to janus structures in Co-Ag nano-islands induced by thermal activation, Phys. Rev. B, submitted
[12] Samant M. G., Bergeret, G. Meitzner, G. Gallezot, P. and Boudart. M. Anomalous wide angle X-ray scattering and X-ray absorption spectroscopy of supported platinum-molybdenum bimetallic clusters. 2. atomic and electronic structure. J. Phys. Chem, 92 :35473554, 1988
[13] Bazin, D. Guczi, L.and Lynch. J. Anomalous wide angle X-ray scattering (AWAXS) and heterogeneous catalysts. Appl. Catal., A, 226, 87, 2002
[14] Andreazza, P., Khelfane, H., Lyon, O. et al. Trends in anomalous small-angle X-ray scattering in grazing incidence for supported nanoalloyed and core-shell metallic nanoparticles. Eur. Phys. J. Spec. Top. 208, 231–244 (2012)